Investigation of Aging Resistance of Asphalts from Different Crude Oils Based on Molecular Structure and Rheological Properties

Zhang, Yichi; Yu, Jianying; Huang, Xiaoqiao; Han, Xiaobin; Xu, Shi; Zou, Yang; Zeng, Shangheng

Yichi Zhang,[1] Jianying Yu,[2] Xiaoqiao Huang,[1,3] Xiaobin Han,[1] Shi Xu,[4] Yang Zou,[1] and Shangheng Zeng[1]

Investigation of Aging Resistance of Asphalts from Different Crude Oils Based on Molecular Structure and Rheological Properties

[1] State Key Laboratory of Silicate Materials for Architectures, Wuhan University of Technology, 122 Luoshi Rd., Wuhan 430070, PR China

[2] State Key Laboratory of Silicate Materials for Architectures, Wuhan University of Technology, 122 Luoshi Rd., Wuhan 430070, PR China (Corresponding author), e-mail: jyyu@whut.edu.cn, https://orcid.org/0000-0002-4096-3907

[3] Research Institute of Petro China Fuel Oil Co. Ltd., 25 Beiwucun Rd., Beijing 100195, PR China (Corresponding author), e-mail: huang-xq@petrochina.com.cn

[4] Hubei Key Laboratory of Roadway Bridge and Structure Engineering, Wuhan University of Technology, 122 Luoshi Rd., Wuhan 430070, PR China; and Civil Engineering and Geosciences, Delft University of Technology, NL-2628 CN Delft, the Netherlands

Reference

ABSTRACT

This research aims to investigate the aging resistance of asphalts from different crude oils based on molecular structure and rheological properties. The average molecular structure of five types of asphalt from different crude oils were analyzed with the element analyzer, nuclear magnetic resonance, gel permeation chromatograph, and the improved Brown–Ladner method. The rheological properties of the asphalts were tested by the dynamic shear rheometer before and after laboratory aging. The antiaging properties of the asphalts were evaluated by the rheological aging index (RAI). The findings indicate that there were significant differences in the molecular structures among the five types of asphalt. The asphalt with the least hydrogen–carbon ratio (H/C), the largest aromatic carbon ratio (f_A), and the largest condensation index (CI) had the lowest rate of decline in rheological properties and therefore, the best antiaging performance. The H/C, f_A, and CI had good correlations with RAI, which indicated that it was feasible to use these molecular structure parameters to evaluate the differences in the aging resistance of various asphalts.

Keywords

Introduction

Asphalt pavement is widely used in the world because of its advantages, such as having no joints, comfort when driving, low noise, wear resistance, short construction period, and

convenient maintenance.[1-3] Within the service life of pavements, asphalt is subject to the long-term coupling effect of heat, oxygen, ultraviolet exposure, and other factors, which leads to performance degradation.[4-6] By conducting aging tests on asphalts at different times, researchers gained a deep understanding of the changes in physical indicators and the decay of properties after aging.[7-9] It is generally believed that various asphalts have different aging resistances but that the law of performance changes are similar.[10] With the increase of aging time, the penetration and ductility of the asphalts decreased, and the softening point increased, while the viscosity, complex shear modulus, and creep stiffness gradually increased.[11-13] This indicates that aging causes asphalt to become more elastic, less temperature sensitive, and less resistant to fatigue cracking, which shortens the service life of the pavement. Therefore, it was necessary to fully understand the aging mechanism of asphalt to improve its aging resistance.

Asphalt is an organic mixture, and its complex aging mechanism has been the focus of researchers' attention.[14-17] Researchers believe that the main causes of asphalt aging are volatilization of light components and internal structural changes (changes in chemical composition and molecular structure caused by oxidation, photopolymerization, and thermal condensation), which also provides some insight into understanding why various asphalts have different aging resistances. Wang and Ye[18] explored the aging properties of asphalts produced from different crude oils and found that the asphalts with the same penetration grade showed different aging resistances. Zhao et al.[19] conducted Thin-Film Oven Test (TFOT) on 18 types of asphalt and found that the aging resistance of asphalt primarily depends on its crude oils. This is because asphalts from different crude oils have dissimilar chemical composition and molecular structures.[20-22]

To investigate how asphalt chemical composition influences aging resistance, Michalica et al.[23] compared the effects of aging on the rheological properties, chemical composition, and molecular structure of two kinds of asphalts from different crude oils and found that the same aging condition produced different effects on these asphalts; namely, the higher the asphaltene content and heteroatom content, the lower the aging sensitivity of the asphalt. Mansourkhaki[24] explored the effect of chemical components on the rheological properties of asphalt before and after aging. It was found that using asphaltene content as an index was more reliable for investigating the effects of aging. Weigel[25] investigated 11 kinds of asphalt samples in different aging states by chemical, rheological, and adhesion-related methods. The results showed that chemical properties have some significant effects on the physical, rheological, aging, and adhesion behavior of the binders and that asphaltenes play a decisive role. However, there was limited research on the relationship between the molecular structure and the aging resistance of asphalts, which is essential to fully understand the aging mechanism and improve the aging resistance of asphalts.

In order to investigate the antiaging properties of asphalts with specific molecular structures, in this paper, the average molecular structures of five kinds of asphalt from different crude oils were analyzed by the element analyzer, nuclear magnetic resonance (NMR), gel permeation chromatograph (GPC), and the improved Brown–Ladner method, respectively. The rheological properties of the asphalts before and after TFOT and pressurized aging vessel (PAV) were tested, and the degradation of rheological properties of asphalts after aging was evaluated by the RAI. Finally, the correlations between the asphalt molecular structure and RAI were established. The research flow diagram of the paper is depicted in figure 1.

Experimental

MATERIALS

Five types of asphalt with a 60/80 penetration grade from different refineries were used in this study, namely, QZ70, GZ70, ZH70, BH70, and HD70. Their physical properties and the processing techniques are listed in Tables 1 and 2, respectively.

AGING METHODS

In order to simulate the aging process in the field in a short time, the TFOT was used to simulate the aging effect of asphalts in the mixing process, and PAV was used to simulate the aging state of pavements operating

FIG. 1 Research flow diagram.

TABLE 1

Physical properties of various asphalts

Sample	Softening Point, °C	Penetration/0.1 mm, 25°C	Viscosity/Pa·s, 60°C
QZ70	49.0	64	250
GZ70	48.7	65	247
ZH70	49.3	65	283
BH70	48.1	70	224
HD70	48.2	80	221

TABLE 2

Processing technique of various asphalts

Sample	Crude Oils	Manufacturing Process
QZ70	Oman	Straight run
GZ70	Saudi Arabia	Blend
ZH70	Cabinda	Straight run
BH70	Suizhong 36-1	Straight run
HD70	Marry-16	Straight run

for 5–10 years. Standardized conditions of 163°C and 5 h were used in TFOT (ASTM D1754, *Standard Test Method for Effects of Heat and Air on Asphaltic Materials (Thin-Film Oven Test)*), and 2.1-MPa air pressure, 100°C, and 20 h after short-term aging were used in PAV (ASTM D6521, *Standard Practice for Accelerated Aging of Asphalt Binder Using a Pressurized Aging Vessel (PAV)*), respectively.

AVERAGE MOLECULAR STRUCTURE CHARACTERIZATION

Element Content

The element analyzer (Vario EL cube, Germany) was used to analyze the content (mass fraction) of carbon, hydrocarbon, nitrogen, and sulfur in the asphalt, and the content of oxygen was obtained by the subtraction method. The element content was used to calculate the average molecular structure of the asphalt.

Hydrogen Atom

^{1}H-NMR (A Bruker AVANCE III HD, Switzerland) was used to detect the hydrogen atoms in asphalt. Deuterated chloroform ($CDCl_3$) was used as the solvent, and 6 mg of asphalt was dissolved into 6 mL of solvent. The test was performed with tetramethylsilane as the internal standard. The different types of hydrogen atoms were divided as shown in Table 3. The chemical shifts of hydrogen atoms were identified in ^{1}H-NMR spectra, and the hydrogen distribution (H_α, H_β, H_γ, and H_{ar}) was calculated.

Average Molecular Weight

The GPC (Waters 1515, U.S.) was used to characterize the molecular weight and distribution of the asphalt. The instrument was equipped with an ultraviolet/visible light detector and a differential refractive index detector. The asphalt was first dissolved into tetrahydrofuran to make the solutions at target concentration (3 mg/mL) and then injected through a 0.2-μm filter to filter out the undissolved impurities. Each sample was tested over a 15-min elution period. The signal of different molecular weight grades was monitored by the detector to obtain the number average molecular weight (M_w), weight average molecular weight (M_n), and molecular weight distribution (Pd) of the asphalt.

Molecular Structure Parameters

The improved Brown–Ladner method proved to be reliable for calculating the molecular structure parameters of the asphalts.[26–28] In order to facilitate comparisons, some structural parameters were selected for calculations, as follows:

$$H/C = \frac{H(\%) \times 12}{C(\%) \times 1} \tag{1}$$

$$C_T = \frac{C(\%) \times M_n}{12} \tag{2}$$

$$H_T = \frac{H(\%) \times M_n}{1} \tag{3}$$

TABLE 3

Types of hydrogen atoms in ^{1}H-NMR spectrum

Types	Chemical Shift, Parts per Million	Attribution
H_{ar}	6.0–9.0	Hydrogen directly linked to aromatic carbon
H_α	2.0–4.0	Hydrogen attached to the C_α of the aromatic ring
H_β	1.0–2.0	Hydrogen on the C_β of the aromatic ring and on the CH_2 and CH groups farther than C_β
H_γ	0.5–1.0	Hydrogen on the C_γ of the aromatic ring and on the CH_3 groups farther than C_γ

$$f_A = \frac{C_T / - \left(\frac{H_\alpha}{H_T} + \frac{H_\beta}{H_T} + H_\gamma / H_T\right)/2}{C_T / H_T} \qquad (4)$$

$$CI = 2 - (H/C) - f_A \qquad (5)$$

where H/C is the molar ratio of hydrogen to carbon, C_T is the total number of carbon atoms, H_T is the total number of hydrogen atoms, f_A is the ratio of the number of aromatic carbon atoms to the total number of carbon atoms, and CI is the condensation degree of ring structure.

The smaller H/C and the larger f_A and CI represented more aromatic ring structures and fewer aliphatic structures in the asphalt, and vice versa.

RHEOLOGICAL PROPERTIES

Dynamic Viscoelastic Properties

A dynamic shear rheometer (MCR-102, Antor Paar, Austria) was adopted to investigate the dynamic viscoelastic properties of the asphalts. The stress-controlled mode was adopted. The test parameters are shown in Table 4.

Repeated Creep Recovery Test

The repeated creep recovery test was used in the research to evaluate the deformation resistance of the asphalts. The test was also performed by a dynamic shear rheometer (DSR) at a stress level at a specified temperature. The shear deformation of the sample in the loading of 1 s and the unloading of 9 s was recorded, and the deformation recovery rate (R) was calculated according to equation (6).

$$R = \frac{\varepsilon_c - \varepsilon_r}{\varepsilon_c - \varepsilon_0} \qquad (6)$$

where ε_0 was the initial value of the strain during the loading phase, ε_c was the strain value at the end of the loading phase, and ε_r was the strain value at the end of the tenth second test.

The asphalts and aged asphalts were tested at 50°C according to AASHTO TP 70-13. The stress level was 0.1 kPa, and the loadings were repeated 10 times.

RAI

In order to further evaluate the influence of aging on the rheological properties of asphalts with different molecular structures, the RAI at specific temperatures, including complex modulus index (CMI), phase angle index (PAI), rutting factor index (RFI), loss tangent index (LTI), and the deformation recovery rate index (RI) of the asphalt were calculated by equations (7)–(11). The RAIs at specific temperatures were selected to compare the differences in the aging resistance of various asphalts in a clear way. The closer the RAI was to 1, the closer the asphalt was to retaining the properties of the original asphalt after aging; that is, the asphalt had better aging resistance.

$$CMI = \frac{G^*_{\text{Aged asphalt}}}{G^*_{\text{Original asphalt}}} \qquad (7)$$

$$PAI = \frac{\delta_{\text{Aged asphalt}}}{\delta_{\text{Original asphalt}}} \qquad (8)$$

TABLE 4

The test parameters of the dynamic viscoelastic properties

	Temperature	Scanning Frequency	Heating Rate	Diameter of Plates	Gap of Plate
High-temperature sweep	30°~80°C	10 rad/s	2°C/min	25 mm	1 mm
Low-temperature sweep	−10°~30°C	10 rad/s	2°C/min	8 mm	2 mm

$$\text{RFI} = \frac{G^*_{\text{Aged asphalt}} \big/ \sin \delta_{\text{Aged asphalt}}}{G^*_{\text{Original asphalt}} \big/ \sin \delta_{\text{Original asphalt}}} \qquad (9)$$

$$\text{LTI} = \frac{\tan \delta_{\text{Aged asphalt}}}{\tan \delta_{\text{Original asphalt}}} \qquad (10)$$

$$\text{RI} = \frac{R_{\text{Aged asphalt}}}{R_{\text{Original asphalt}}} \qquad (11)$$

Results and Discussion

AVERAGE MOLECULAR STRUCTURE OF ASPHALTS

The element composition of asphalts is shown in **Table 5**. It can be seen from **Table 5** that except for the similar content of carbon, the contents of other elements were quite diverse.

Different hydrogen atom contents of the asphalts from ^{1}H-NMR are shown in **Table 6**. In **Table 6**, it can be found that there were significant differences in the contents of hydrogen atoms in asphalts produced from

TABLE 5

The element composition of asphalts

Element Content, wt %	QZ70	GZ70	ZH70	BH70	HD70
C	83.35	82.89	82.04	83.37	82.55
H	9.31	10.34	10.34	10.90	11.08
N	0.50	0.47	0.45	0.81	0.79
S	5.23	5.17	6.17	3.25	4.26
O	0.96	0.75	0.87	1.20	1.31

TABLE 6

Different hydrogen atom content of asphalts

	QZ70	GZ70	ZH70	BH70	HD70
H_α	0.019	0.095	0.021	0.014	0.234
H_β	0.690	0.706	0.700	0.816	0.378
H_γ	0.234	0.182	0.261	0.144	0.332
H_{ar}	0.016	0.018	0.018	0.026	0.056

TABLE 7

M_n, M_w, and Pd of asphalts

	QZ70	GZ70	ZH70	BH70	HD70
M_n	742	716	664	640	649
M_w	1,004	975	851	833	910
Pd	1.35	1.36	1.28	1.30	1.38

TABLE 8

The average molecular structure of asphalts

	QZ70	GZ70	ZH70	BH70	HD70
H/C	1.340	1.497	1.512	1.569	1.611
f_A	0.368	0.265	0.258	0.236	0.202
CI	0.292	0.238	0.23	0.195	0.187

FIG. 2 Complex modulus of all samples at the temperature of 30°~80°C; (*A*) original; (*B*) TFOT; (*C*) PAV.

(*A*)

(*B*)

(*C*)

FIG. 3

CMI of asphalt with different molecular structure under the conditions of TFOT and PAV aging at a temperature of 40°C.

FIG. 4 Phase angle of all samples at the temperature of 30°~80°C; (*A*) original; (*B*) TFOT; (*C*) PAV.

(*A*)

(*B*)

(*C*)
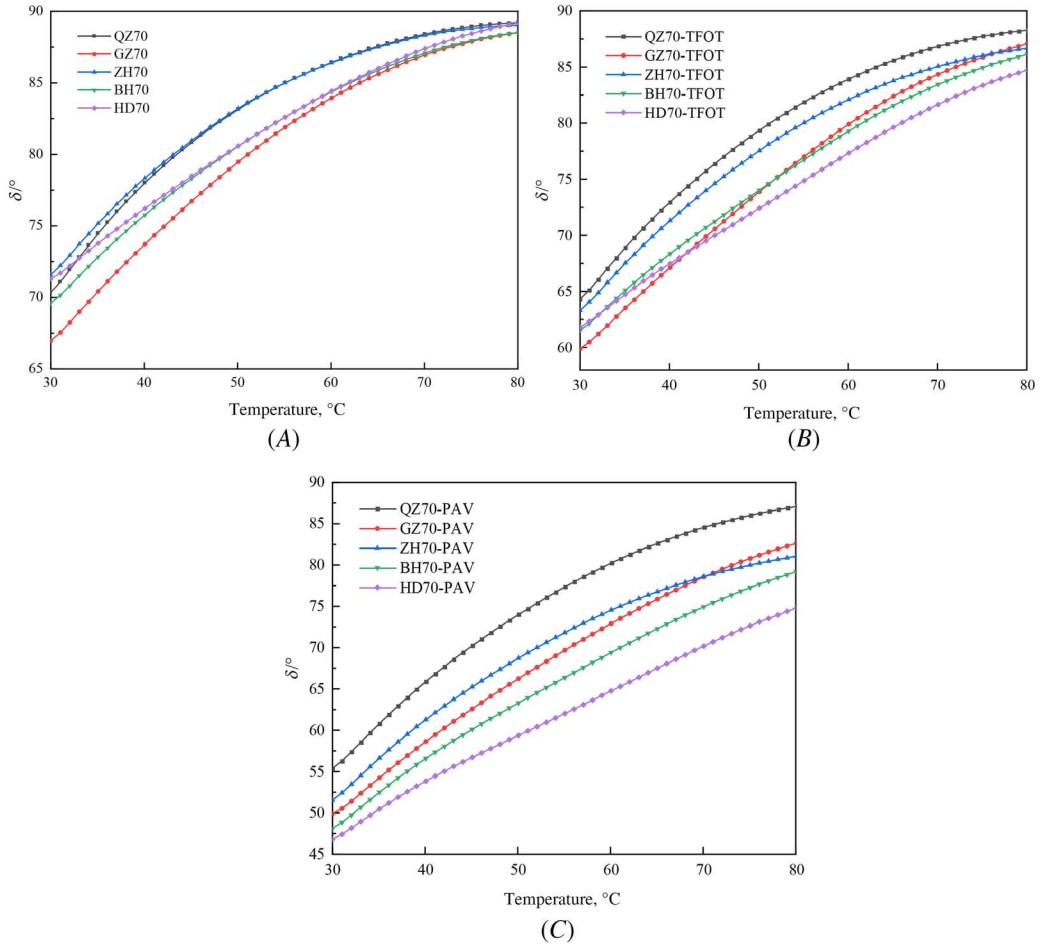
FIG. 5

PAI of asphalts with different molecular structure under the conditions of TFOT and PAV aging at a temperature of 40°C.
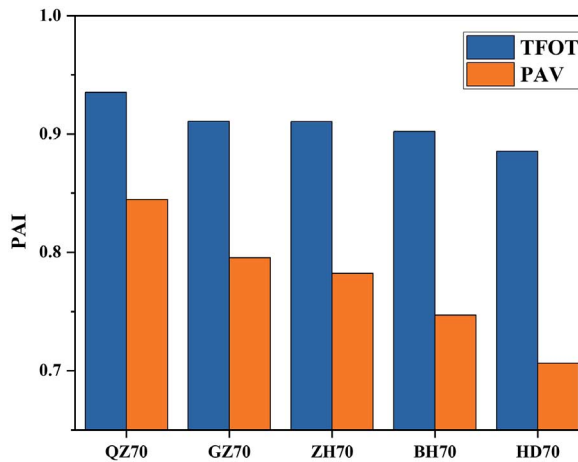
different crude oils. Among the four kinds of hydrogen atoms, the content of H_β had the most content, followed by H_γ and then H_α, with H_{ar} having the least.

The M_n, M_w, and Pd of asphalts from the GPC is shown in **Table 7**. It can be seen from the molecular weight results (**Table 7**) that the molecular weights of the five asphalts and their distributions differed greatly. The QZ70 has the largest molecular weight, and BH70 has the smallest molecular weight.

The average molecular structures of the asphalts, calculated using the improved Brown–Ladner method, are listed in **Table 8**. The hydrogen–carbon ratio (H/C), aromatic carbon ratio (f_A), and condensation index (CI) were also different. Among the five types of asphalt, the H/C of all asphalts from small to large sequencing was followed by QZ70, GZ70, ZH70, BH70, and HD70. The ranking of f_A and CI was HD70 < BH70 < ZH70 < GZ70 < QZ70. The QZ70 had the smallest H/C and the largest f_A and CI, which were 1.340, 0.368, and 0.292, respectively. The HD70 had the largest H/C and the smallest f_A and CI, which were 1.611, 0.202, and 0.187, respectively. This shows that QZ70 had the most aromatic ring structures and minimal aliphatic structures and that HD70 had minimal aromatic ring structures and the most aliphatic structures to some extent.

FIG. 6 Rutting factor of all samples at the temperature of 30°~80°C; (A) original; (B) TFOT; (C) PAV.
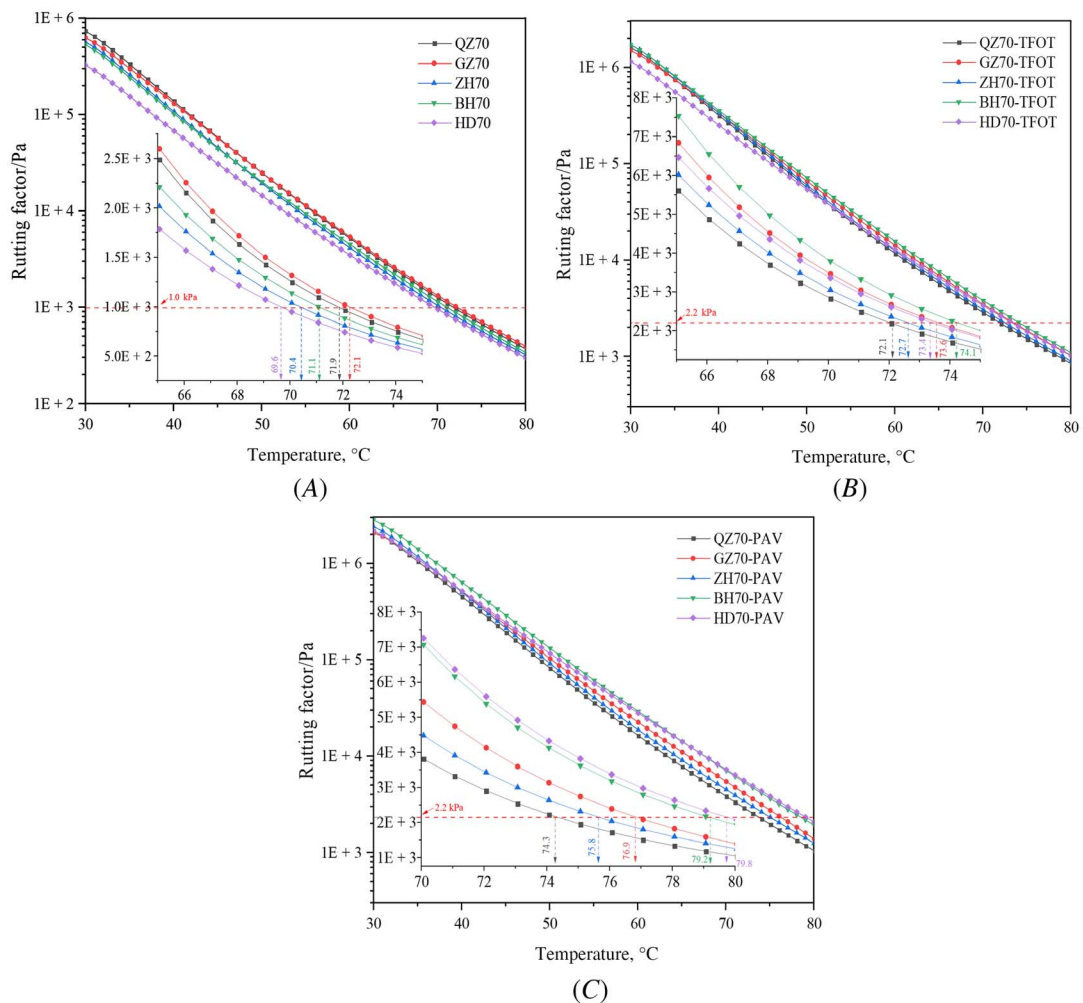
HIGH-TEMPERATURE RHEOLOGICAL PROPERTIES OF ASPHALTS BEFORE AND AFTER AGING

Complex Modulus

The complex modulus (G^*) was used to represent the measure of the material's total resistance to deformation under repeated shear stress load. The larger the complex modulus of the asphalt was, the better the shear deformation resistance was. The relationship between temperature and complex modulus of asphalts with different molecular structures under different aging conditions is shown in figure 2. Figure 2A shows that there were differences in the complex modulus of five kinds of asphalt before aging. At 40°C, the G^* of the five asphalts were 1.33×10^5 Pa, 1.25×10^5 Pa, 1.05×10^5 Pa, 9.90×10^4 Pa, and 6.50×10^4 Pa, respectively, which was double the difference. Figure 2B and 2C shows that the G* of asphalts increased significantly after aging. However, the variation rule of complex modulus of different asphalts under the same aging condition was diverse, reflecting the difference of aging resistance of asphalts with different molecular structures.

In order to clearly compare the differences in antiaging properties due to molecular structures, the CMI of asphalts with different molecular structures at 40°C under the conditions of TFOT and PAV aging and calculated by equation (7) is shown in figure 3. It can be seen from figure 3 that the CMI of the five asphalts are in the following order: HD70 > BH70 > ZH70 > GZ70 > QZ70 > 1. It shows that QZ70 (with the least H/C, the largest f_A, and the largest CI) has the best resistance to shear deformation, whereas HD70 (with the largest H/C,

FIG. 7

RFI of asphalts with different molecular structures under the conditions of TFOT and PAV aging at the temperature of 40°C.
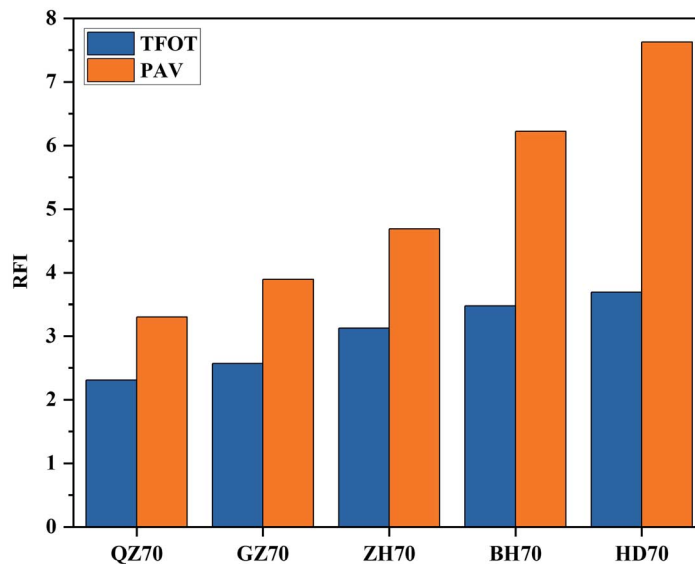
TABLE 9

The RCT of all samples

Sample	RCT, °C			ΔRCT, °C	
	Original	TFOT	PAV	TFOT	PAV
QZ70	71.9	72.1	74.3	0.2	2.4
GZ70	72.1	73.6	76.9	1.5	4.8
ZH70	70.4	72.7	75.8	2.3	5.4
BH70	71.1	74.1	79.2	3.0	8.1
HD70	69.6	73.4	79.8	3.8	10.2

the least f_A, and the least CI) was the worst. The mechanism could be that with the increase of f_A and CI and the decrease of H/C, the aromatic ring structure in the asphalt was more complex and the number of aromatic rings increased, resulting in an increase of rigidity and decrease of flexibility in the internal molecules, which were less prone to mutual displacement between molecules. As a result, the elasticity of the asphalt increased, the viscosity decreased, the resistance to external loading increased, and the flow deformation was less likely to occur under the action of external forces. At the same time, it also hindered the occurrence of some aging reactions and the volatilization of small molecules. Therefore, the asphalt with higher f_A and CI and less H/C exhibited better aging resistance.

Phase Angle

The phase angle reflects the relative proportions of the elastic and viscous components of the asphalt. The larger the δ was, the higher the viscosity ratio of the asphalt. The asphalt produced more plastic deformation under stress and was more prone to rutting at high temperatures. **Figure 4** shows the relationship between temperature and the δ of asphalts with different molecular structures under different aging conditions. With the increase of temperature, the δ of all asphalts increased gradually. **Figure 4A** shows that the δ of asphalts with different molecular structures before aging are different. The molecular structure of an asphalt also

FIG. 8 Complex modulus of all samples at a temperature of −10°~30°C; (*A*) original; (*B*) TFOT; (*C*) PAV.
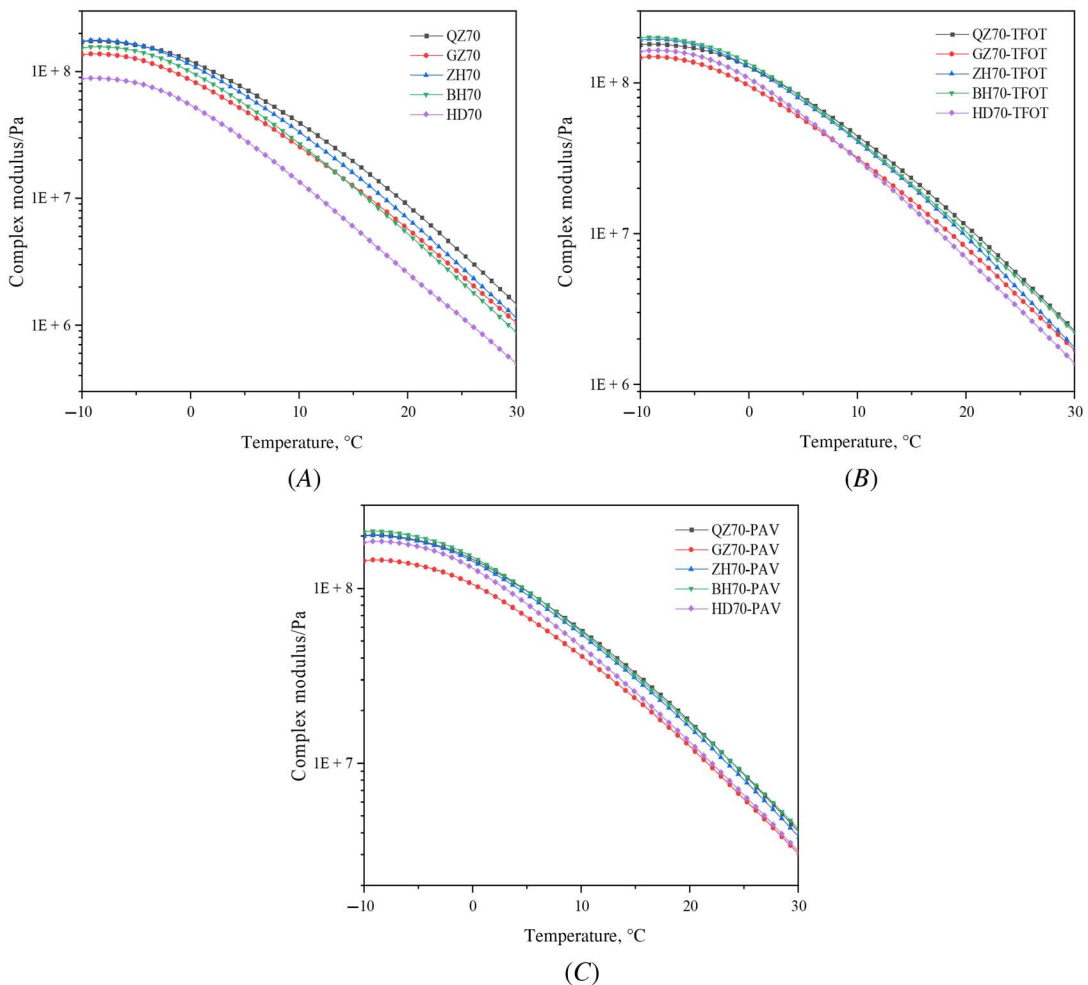
affected the ratio of its viscous components to elastic components. Among the five types of asphalt, the δ at 40°C was 78.3°, 78.0°, 76.2°, 75.8°, and 73.7°, respectively, and the difference between the maximum and minimum was 4.6°. **Figure 4B** and **4C** shows that the δ of asphalt decreases greatly after aging, which indicates that aging could promote the transformation from viscous component to elastic component in asphalt.

The PAI of asphalts with different compositions at 40°C, calculated by equation (8), is shown in **figure 5**. It shows that the PAI of the five asphalts were in the following order: HD70 < BH70 < ZH70 < GZ70 < QZ70 < 1. Therefore, QZ70 had the best antiaging ability, which is consistent with the conclusion obtained from complex modulus. The increase in f_A and CI led to an increase in stiffness and a decrease in the flexibility of the asphalts, which resulted in a decrease in δ for the asphalts.

Rutting Factor

Following the standard Strategic Highway Research Program (SHRP), the rutting factor ($G^*/\sin\delta$) of asphalts can be used to characterize the antirutting deformation ability of the asphalt binder. The larger the value, the stronger the antirutting deformation ability, and vice versa. The $G^*/\sin \delta$ of asphalts with different molecular structures before and after aging are plotted in **figure 6**. It was clear that with the increase in temperature, the $G^*/\sin\delta$ of all samples presented a decreasing trend. By calculating the RFI (**fig. 7**), the change rate of $G^*/\sin\delta$ after aging was obtained: HD70 > BH70 > ZH70 > GZ70 > QZ70 > 1.

The rutting critical temperature (RCT) when $G^*/\sin \delta$ reached 1 kPa and 2.2 kPa, respectively, before and after aging was regarded as the highest service temperature of the asphalt. To further verify the previous conclusion, the RCTs and ΔRCTs (increment of RCT) of all samples are listed in **Table 9**. Before aging, the RCTs of the five asphalts were 69.6°C, 70.4°C, 71.1°C, 71.9°C, and 72.1°C. After aging, the RCTs were increased to varying degrees. The results show that aging had the weakest effect on QZ70.

LOW-TEMPERATURE RHEOLOGICAL PROPERTIES OF ASPHALTS BEFORE AND AFTER AGING

Complex Modulus

Figure 8 shows the complex modulus of asphalt samples before and after aging at −10°~30°C. Before aging, the complex modulus of five kinds of asphalt at 0°C was 1.24×10^8 Pa, 1.17×10^8 Pa, 1.03×10^8 Pa, 8.85×10^7 Pa, and

FIG. 9

CMI of asphalts with different molecular structure under the conditions of TFOT and PAV aging at a temperature of 0°C.
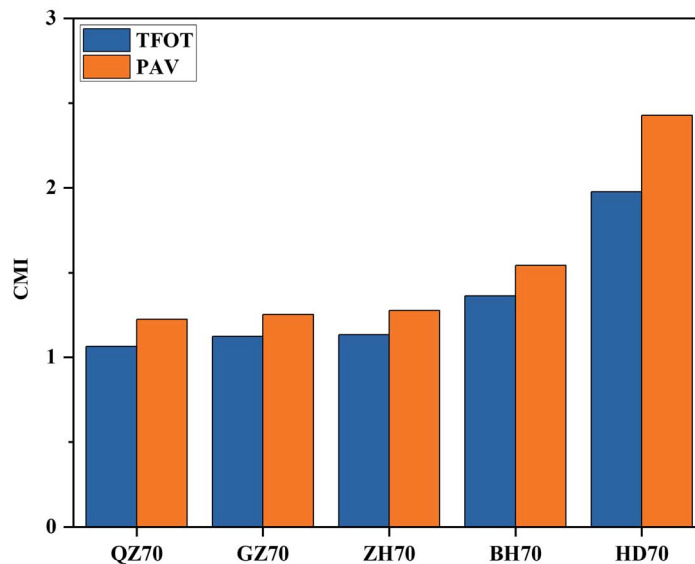
5.65×10^7 Pa, respectively. By comparing the complex modulus of five kinds of asphalt before and after aging, it was found that different samples still show different changes under the same aging conditions. The calculated CMI at a low temperature is shown in **figure 9**. It is seen from **figure 9** that the CMI of the five asphalts were in the following order: HD70 > BH70 > ZH70 > GZ70 > QZ70 > 1. It shows that QZ70 (with the least H/C, the largest f_A, and the largest CI) also had the best resistance to shear deformation at a low temperature among the five kinds of asphalt.

Phase Angle

Figure 10 plots the δ of different asphalt samples at a low temperature. It is shown by **figure 10** that asphalt samples had a higher phase angle at a low temperature. The proportion of elastic component increased at low temperature, and the recovery ability became better after deformation. Before aging, the δ at 0°C was 25.4°, 26.4°, 29.2°, 29.4°, and 33.7°, respectively. The difference between different asphalts reached 8.3°, which was greater than that at 40°C. The PAI of asphalts with different molecular structures under different aging conditions at 0°C is shown in **figure 11**. QZ70 with lower H/C and higher f_A and CI had a phase angle closer to the original asphalt than other asphalts.

FIG. 10   Phase angle of all samples at a temperature of −10°~30°C; (*A*) original; (*B*) TFOT; (*C*) PAV.

FIG. 11

PAI of asphalts with different molecular structure under the conditions of TFOT and PAV aging at the temperature of 0°C.

FIG. 12 Loss tangent of all samples at a temperature of −10°~30°C; (*A*) original; (*B*) TFOT; (*C*) PAV.
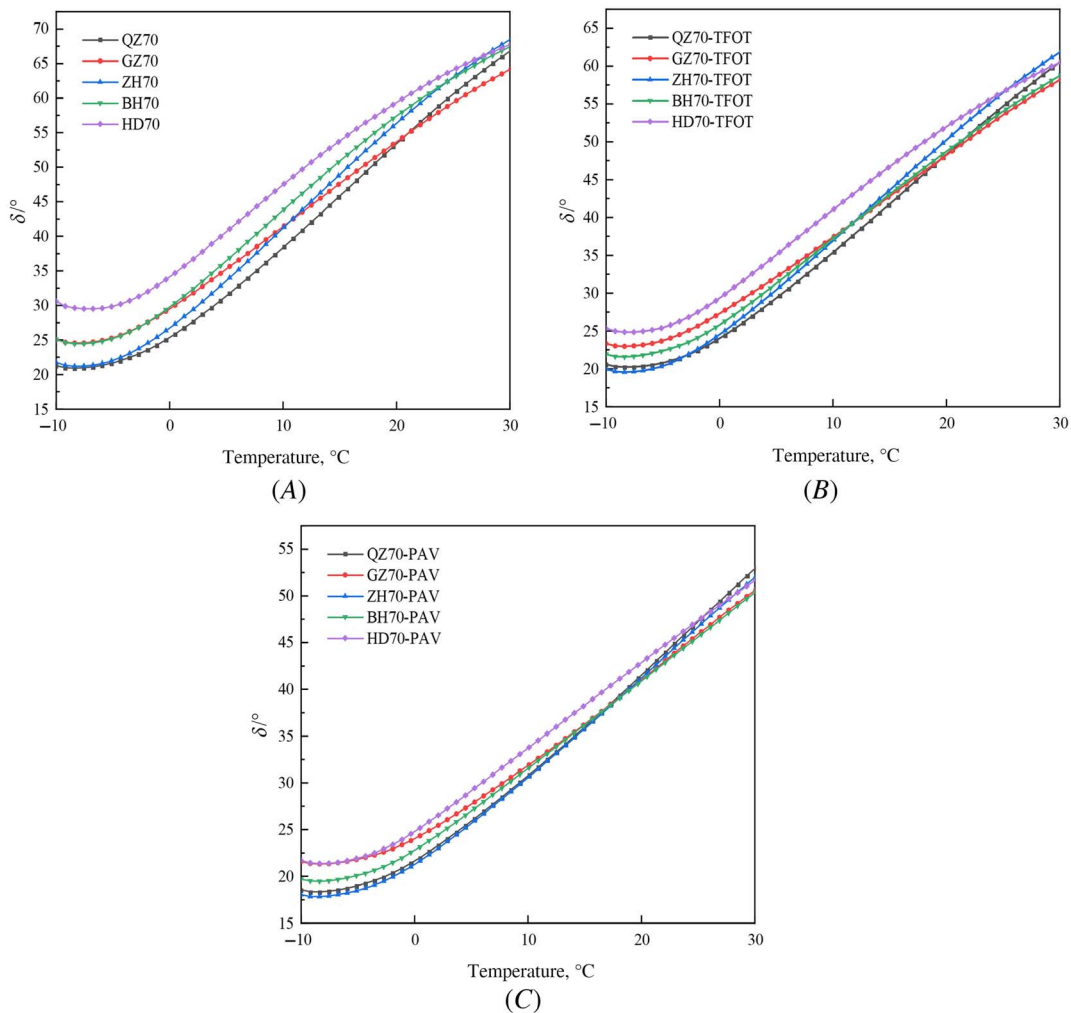
Loss Tangent

Loss tangent (tan δ) is the ratio of loss modulus and storage modulus of an asphalt. It describes the ratio of viscous component and elastic component of an asphalt and is often used to characterize the viscoelastic properties of asphalt. **Figure 12** shows tan δ of different asphalts before and after aging. It can be seen from **figure 12** that the tan δ of each asphalt sample increases in varying degrees with the increase of temperature. During the aging process, asphalt hardens because of aging; the loss modulus (viscous component) of the asphalt decreases rapidly, while the storage modulus (elastic component) increases. The variation (from **fig. 13**) of loss factors of different asphalts was similar to the conclusion obtained from the aforementioned test. The asphalt with rich aromatic rings has good aging resistance.

REPEATED CREEP RECOVERY PROPERTIES OF ASPHALTS BEFORE AND AFTER AGING

Repeated creep and recovery tests can effectively simulate the strain mode of pavements under practice loading, which can reflect the viscoelastic properties of asphalts. **Figure 14** displays the repeated creep and recovery curves of all samples in 10 cycles at a temperature of 50°C. **Figure 15A** shows the R of asphalts with different molecular structures under different aging conditions at 50°C. It can be seen that the strain of the asphalt increases with the increase of action time. With the deepening of aging degree, the strain R of asphalt increases, indicating that aging can promote the internal viscous components of an asphalt to transform to elasticity. The R of the five kinds of asphalts were 4.6 %, 5.4 %, 7.5 %, 8.7 %, and 9.8 %, which increased to 5.1 %, 7.4 %, 11.8 %, 14.6 %, and 23.3 % after TFOT, respectively, and increased to 15.2 %, 15.8 %, 26.5 %, 31.97 %, and 44.2 % after PAV. This is because aging leads to an increase in the content of polar chemical functional groups, such as carbonyl and subpeak groups in the asphalt, and an increase in molecular weight. As a result, the rigidity of the asphalt was increased. Under the action of external forces, only bond rotation and intermolecular cross-linking occurred in the molecular structure of the asphalts, while intermolecular slip was reduced. This allowed the asphalt to remain in its original state for a certain period of time, increasing the strain recovery rate.

The RI of various asphalts under different aging conditions is shown in **figure 15B**. It can be seen from **figure 15B** that the RI of the five asphalts was in the following order: HD70 > BH70 > ZH70 > GZ70 > QZ70 > 1, which indicates that QZ70 with lower H/C and a higher f_A and CI had the closest permanent deformation resistance to the original asphalt and the best antiaging performance.

FIG. 13

LTI of asphalts with different molecular structure under the conditions of TFOT and PAV aging at the temperature of 0°C.
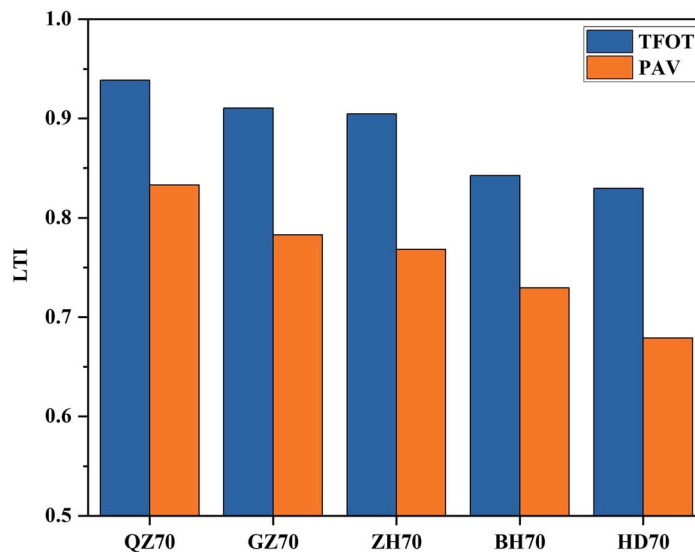
FIG. 14   Repeated creep and recovery property of all samples at 50°C; (*A*) original; (*B*) TFOT; (*C*) PAV.
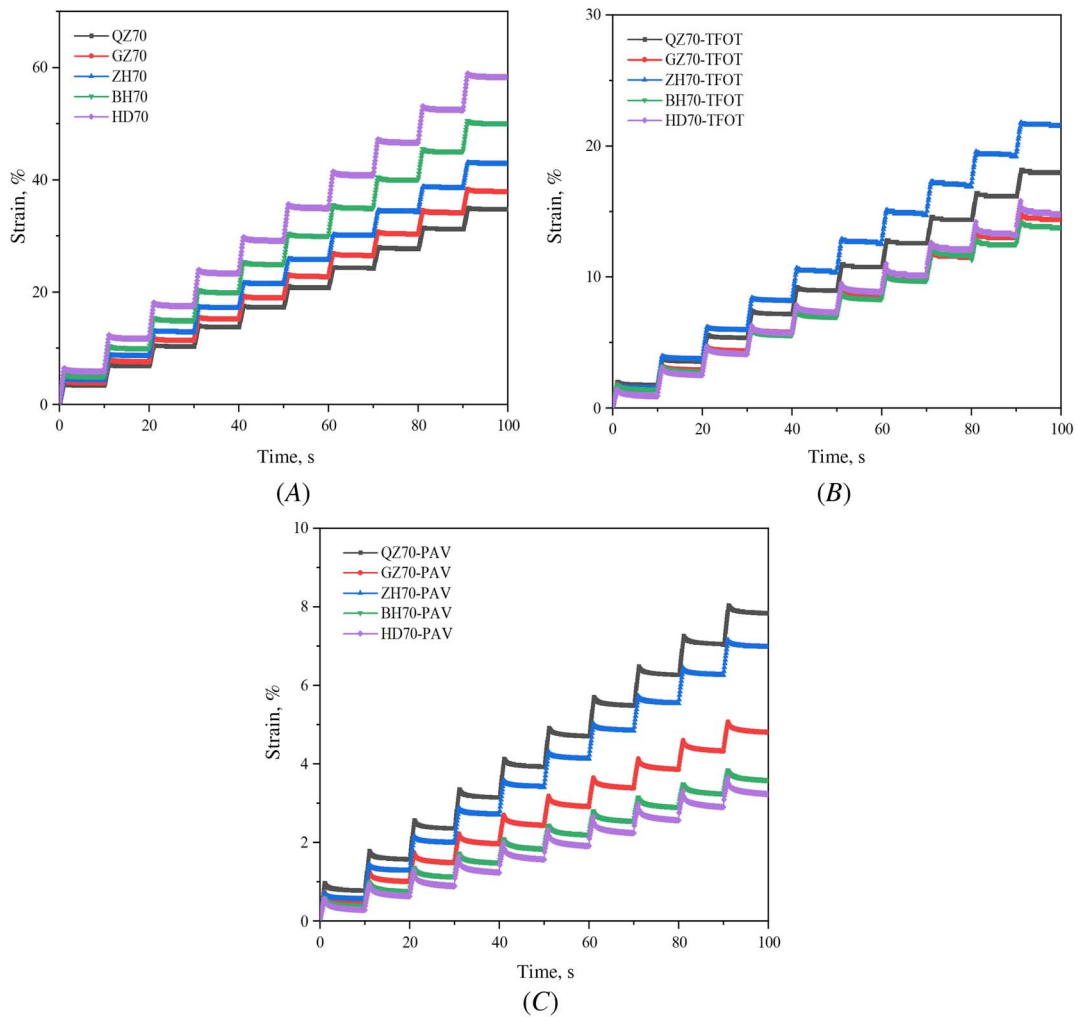
CORRELATION OF RAI AND MOLECULAR STRUCTURE OF ASPHALTS

In order to investigate the effects of different molecular structure on the aging properties of asphalts, the relationship between the hydrogen–carbon ratio/f_A/CI and RAIs is established in this research. A positive correlation represented more molecular structure content with a larger RAI, and the negative correlation represented more molecular structure content with a smaller RAI. The absolute value of the correlation coefficient was closer to 1, which means the correlation was stronger. A relationship was established to verify the feasibility of using the average molecular structure to research the aging resistance of different asphalts. Origin Pro 8.0 was used for a Pearson correlation analysis with a bilateral confidence level of 0.05.

The correlations between the molecular structure (including H/C, f_A, and CI) and the RAI of asphalts are shown in the Table 10. According to the Pearson correlation coefficient in Table 10, three kinds of molecular structure characteristics had a good correlation with the RAI. Taken overall, the CI had the highest correlation, followed by H/C and f_A. The correlation coefficients of the CI and the RAI reached above 0.910 under both TFOT and PAV conditions, and the correlation coefficients for all other structural parameters and the RAI also reached above 0.840, except for the CMI at 0°C. For the RAI, the high-temperature rheological properties of asphalts had the highest correlation with

FIG. 15 R and RI of asphalts with different molecular structure under the conditions of TFOT and PAV aging at 50°C; (A) R; (B) RI.
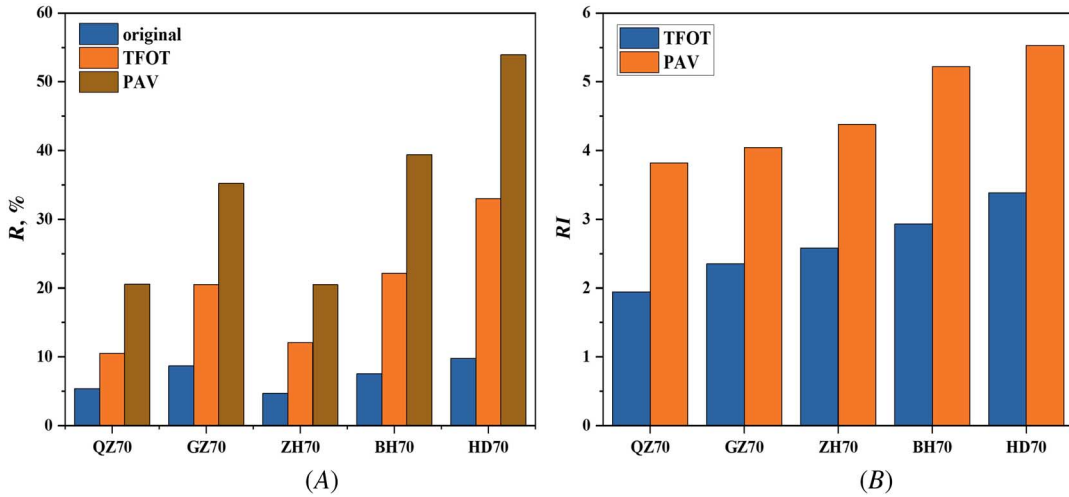
TABLE 10
The result of the calculated Pearson correlation coefficient

Molecular Structure	Aging Condition	Dynamic Viscoelastic Properties						Creep Recovery
		40°C			0°C			50°C
		CMI	PAI	RFI	CMI	PAI	LTI	RI
H/C	TFOT	0.905	−0.978	0.915	0.734	−0.901	−0.904	0.942
	PAV	0.878	−0.962	0.881	0.697	−0.956	−0.949	0.878
f_A	TFOT	−0.876	0.978	−0.887	−0.719	0.861	0.867	−0.924
	PAV	−0.847	0.948	−0.851	−0.683	0.939	0.935	−0.840
CI	TFOT	−0.934	0.962	−0.943	−0.745	0.947	0.946	−0.954
	PAV	−0.911	0.969	−0.911	−0.706	0.965	0.957	−0.922

molecular structures, followed by the creep recovery properties and the low-temperature rheological properties. The results of the correlation analysis exhibited the same experimental conclusion as the rheological experiments; i.e., the asphalt exhibited better aging resistance with decreasing H/C and increasing f_A and CI. Therefore, it was feasible to use these three molecular structure parameters to evaluate the differences in the aging resistance of various asphalts.

Conclusions

In this paper, the average molecular structures of five types of asphalt from different crude oils were analyzed. The rheological properties of the asphalts before and after aging were tested. The correlations between molecular structure and RAI were established. The conclusions were as follows:

(1) There were significant differences in the molecular structure of asphalts from different crude oils. Among five kinds of asphalt, the H/C, f_A, and CI of asphalts ranged from 1.340–1.611, 0.202–0.368, and 0.187–0.292, respectively. The QZ70 had the smallest H/C, the largest f_A and CI, and the HD70 had the largest H/C and the smallest f_A and CI. It showed that QZ70 had the most aromatic ring structures and a minimal aliphatic structure, whereas HD70 had minimal aromatic ring structures and the most aliphatic structure to some extent.

(2) High- and low-temperature dynamic viscoelastic performance of various asphalts showed that the QZ70, with the least H/C, largest f_A, and largest CI, had the RAIs closest to 1; i.e., the asphalt had the lowest rate of decline in rheological properties, which meant it had the best antiaging properties. Meanwhile, the HD70, with the largest H/C and the least f_A and CI, had the RAIs furthest from 1, which means it had the worst antiaging properties.

(3) Repeated creep recovery tests showed that various asphalts had different recovery rates before and after aging. The R of the original asphalt was 4.5∼10 %, which increased to 10∼34 % after TFOT and increased to 20∼54 % after PAV. The RI showed that the RI of QZ70 with the least H/C and the largest f_A and CI was closer to 1, showing better antiaging performance.

(4) According to the Pearson correlation coefficient, the three kinds of molecular structures of asphalts had good correlations with RAIs, and the correlation between CI and RAI was the best, followed by H/C and f_A. For the RAI, the high-temperature rheological properties of asphalts had the highest correlation with molecular structures, followed by the creep recovery properties and the low-temperature rheological properties.

ACKNOWLEDGMENTS

References

1. Y. Cheng, J. Tao, Y. Jiao, G. Tan, Q. Guo, S. Wang, and P. Ni, "Influence of the Properties of Filler on High and Medium Temperature Performances of Asphalt Mastic," *Construction and Building Materials* 118 (August 2016): 268–275, https://doi.org/10.1016/j.conbuildmat.2016.05.041

2. S. Xu, X. Liu, A. Tabaković, and E. Schlangen, "A Novel Self-Healing System: Towards a Sustainable Porous Asphalt," *Journal of Cleaner Production* 259 (June 2020): 120815, https://doi.org/10.1016/j.jclepro.2020.120815

3. J.-S. Chen, S.-F. Chen, and M.-C. Liao, "Physical and Chemical Properties of Asphalts Associated with Performance," *Journal of Testing and Evaluation* 42, no. 5 (September 2014): 1081–1088, https://doi.org/10.1520/JTE20130195

4. V. Mouillet, F. Farcas, and S. Besson, "Ageing by UV Radiation of an Elastomer Modified Bitumen," *Fuel* 87, no. 12 (September 2008): 2408–2419, https://doi.org/10.1016/j.fuel.2008.02.008

5. A. Shenoy, "Prediction of High Temperature Rheological Properties of Aged Asphalts from the Flow Data of the Original Unaged Samples," *Construction and Building Materials* 16, no. 8 (December 2002): 509–517, https://doi.org/10.1016/S0950-0618(02)00030-2

6. Q. Qin, J. F. Schabron, R. B. Boysen, and M. J. Farrar, "Field Aging Effect on Chemistry and Rheology of Asphalt Binders and Rheological Predictions for Field Aging," *Fuel* 121 (April 2014): 86–94, https://doi.org/10.1016/j.fuel.2013.12.040

7. P. Cong, J. Wang, K. Li, and S. Chen, "Physical and Rheological Properties of Asphalt Binders Containing Various Antiaging Agents," *Fuel* 97 (July 2012): 678–684, https://doi.org/10.1016/j.fuel.2012.02.028

8. H. Zhang, Z. Chen, G. Xu, and C. Shi, "Evaluation of Aging Behaviors of Asphalt Binders through Different Rheological Indices," *Fuel* 221 (June 2018): 78–88, https://doi.org/10.1016/j.fuel.2018.02.087

9. D. Li, Z. Leng, F. Zou, and H. Yu, "Effects of Rubber Absorption on the Aging Resistance of Hot and Warm Asphalt Rubber Binders Prepared with Waste Tire Rubber," *Journal of Cleaner Production* 303 (June 2021): 127082, https://doi.org/10.1016/j.jclepro.2021.127082

10. I. G. do Nascimento Camargo, B. Hofko, J. Mirwald, and H. Grothe, "Effect of Thermal and Oxidative Aging on Asphalt Binders Rheology and Chemical Composition," *Materials* 13, no. 19 (October 2020): 4438, https://doi.org/10.3390/ma13194438

11. X. Hou, F. Xiao, J. Wang, and S. Amirkhanian, "Identification of Asphalt Aging Characterization by Spectrophotometry Technique," *Fuel* 226 (August 2018): 230–239, https://doi.org/10.1016/j.fuel.2018.04.030

12. M. Guo, X. Liu, Y. Jiao, Y. Tan, and D. Luo, "Rheological Characterization of Reversibility between Aging and Rejuvenation of Common Modified Asphalt Binders," *Construction and Building Materials* 301 (September 2021): 124077, https://doi.org/10.1016/j.conbuildmat.2021.124077

13. H. Zhang, Z. Chen, G. Xu, and C. Shi, "Physical, Rheological and Chemical Characterization of Aging Behaviors of Thermochromic Asphalt Binder," *Fuel* 221 (January 2018): 850–858, https://doi.org/10.1016/j.fuel.2017.09.111

14. J. C. Petersen and R. Glaser, "Asphalt Oxidation Mechanisms and the Role of Oxidation Products on Age Hardening Revisited," *Road Materials and Pavement Design* 12, no. 4 (December 2011): 795–819, https://doi.org/10.1080/14680629.2011.9713895

15. T. Ma, X. Huang, Y. Zhao, and H. Yuan, "Aging Behaviour and Mechanism of SBS-Modified Asphalt," *Journal of Testing and Evaluation* 40, no. 7 (December 2012): 1186–1191, https://doi.org/10.1520/JTE20120150

16. L. Luo, L. Chu, and T. F. Fwa, "Molecular Dynamics Analysis of Oxidative Aging Effects on Thermodynamic and Interfacial Bonding Properties of Asphalt Mixtures," *Construction and Building Materials* 269 (February 2021): 121299, https://doi.org/10.1016/j.conbuildmat.2020.121299

17. W. Ye, W. Jiang, P. Li, D. Yuan, J. Shan, and J. Xiao, "Analysis of Mechanism and Time-Temperature Equivalent Effects of Asphalt Binder in Short-Term Aging," *Construction and Building Materials* 215 (August 2019): 823–838, https://doi.org/10.1016/j.conbuildmat.2019.04.197

18. Z. Wang and F. Ye, "Experimental Investigation on Aging Characteristics of Asphalt Based on Rheological Properties," *Construction and Building Materials* 231 (January 2020): 117158, https://doi.org/10.1016/j.conbuildmat.2019.117158

19. P. Zhao, D. Gao, R. Ren, K. Han, Z. Yang, W. Meng, and W. Fan, "Short-Term Aging Performance Evaluation of Asphalt Based on Principal Component and Cluster Analysis," *Journal of Testing and Evaluation* 49, no. 1 (May 2019): 590–602, https://doi.org/10.1520/JTE20180781

20. R. Ren, W. Fan, P. Zhao, H. Zhou, W. Meng, and P. Ji, "Crude Oil Source Identification of Asphalt via ATR-FTIR Approach Combined with Multivariate Statistical Analysis," *Advances in Materials Science and Engineering* 2020 (July 2020): 1–13, https://doi.org/10.1155/2020/2025072

21. C. Varanda, I. Portugal, J. Ribeiro, A. M. S. Silva, and C. M. Silva, "Influence of Polyphosphoric Acid on the Consistency and Composition of Formulated Bitumen: Standard Characterization and NMR Insights," *Journal of Analytical Methods in Chemistry* 2016 (August 2016): 803–832, https://doi.org/10.1155/2016/2915467

22. Y. Edwards and P. Redelius, "Rheological Effects of Waxes in Bitumen," *Energy & Fuels* 17, no. 3 (May 2003): 511–520, https://doi.org/10.1021/ef020202b

23. P. Michalica, I. B. Kazatchkov, J. Stastna, and L. Zanzotto, "Relationship between Chemical and Rheological Properties of Two Asphalts of Different Origins," *Fuel* 87, nos. 15–16 (November 2008): 3247–3253, https://doi.org/10.1016/j.fuel.2008.05.021

24. A. Mansourkhaki, M. Ameri, M. Habibpour, and B. S. Underwood, "Chemical Composition and Rheological Characteristics of Binders Containing RAP and Rejuvenator," *Journal of Materials in Civil Engineering* 32, no. 4 (April 2020): 04020026, https://doi.org/10.1061/(ASCE)MT.1943-5533.0003016

25. S. Weigel and D. Stephan, "Relationships between the Chemistry and the Physical Properties of Bitumen," *Road Materials and Pavement Design* 19, no. 7 (June 2017): 1636–1650, https://doi.org/10.1080/14680629.2017.1338189

26. Q. Wang, C. Jia, J. Ge, and W. Guo, "^{1}H NMR and ^{13}C NMR Studies of Oil from Pyrolysis of Indonesian Oil Sands," *Energy & Fuels* 30, no. 3 (March 2016): 2478–2491, https://doi.org/10.1021/acs.energyfuels.5b01215

27. Y. Gong, J. Xu, and E.-H. Yan, "Intrinsic Temperature and Moisture Sensitive Adhesion Characters of Asphalt-Aggregate Interface Based on Molecular Dynamics Simulations," *Construction and Building Materials* 292 (July 2021): 123462, https://doi.org/10.1016/j.conbuildmat.2021.123462

28. M. Guo, M. Liang, Y. Fu, A. Sreeram, and A. Bhasin, "Average Molecular Structure Models of Unaged Asphalt Binder Fractions," *Materials and Structures* 54, no. 173 (August 2021): 1–18, https://doi.org/10.1617/s11527-021-01754-2